IEEE Transactions on Nuclear Science, Vol. NS-34, No. 6, December 1987

EXTENDED PHOTOCURRENT MODELING WITH APPLICATION TO LATCHUP ANALYSIS

A. Ishaque, M. Becker, R. C. Block
Gaerttner Linear Accelerator Laboratory
Rensselaer Polytechnic Institute
Troy, NY 12180-3590

ABSTRACT

Nonlinear departure from low injection and bipolar device modeling are introduced into TRISPICE. These features and other advanced aspects of TRISPICE photocurrent representation are found to be significant for study of latchup.

INTRODUCTION

It has been customary to model circuit behavior in the presence of transient ionizing radiation by placing precalculated transient current sources at the various nodes in the circuit where photocurrents are generated. Circuit simulation codes like SPICE[1] have been used in this manner for upset as well as latchup analysis[2]. Photocurrent produced in an ohmic field free pn junction device is given by the well known model of Wirth and Rogers[3] for low level injection situations. A photocurrent source implementing this model has been incorporated in a version of SPICE called TRISPICE[4] with extensions for 3-D geometry and finite device dimensions. The photocurrent source in TRISPICE is tailored to the specific geometry of the CMOS configuration.

This paper first reports on extended model for photocurrent which explicitly takes into account non-linear recombination and diffusion processes arising as a result of departure from low level injection. For an n-type material, if we take the electron concentration $n_o = 10^{16}$ cm^{-3}, and minority carrier lifetime $\tau_{po} = 10^{-7}$ sec, then $(\tau_{po} G)/n_o = 0.4$ at $\dot{\gamma} = 10^9$ rads/sec (low level injection requires $(\tau_{po} G)/n_o \ll 1$). Thus departure from low injection can be of concern at moderate dose-rates. The implementation of this extended model into TRISPICE is then described. The last section of the paper describes the results of latchup modeling using TRISPICE and compares and contrasts the approach with conventional SPICE modeling. The nonlinear photocurrent source is also applied to latchup analysis and the results are compared with the results obtained by using the linear photocurrent source.

NONLINEAR PHOTOCURRENT MODELING

In the presence of a carrier generation rate G, the excess carrier concentration (δp) in a n-type semiconductor is given by

$$\frac{\partial \delta p}{\partial t} = D_a \frac{\partial^2 \delta p}{\partial x^2} - \mu_a E \frac{\partial \delta p}{\partial x} + G - U \qquad (1)$$

where E is the electric field in the quasi-neutral region, and

$$D_a = \frac{(n + p)\, D_n D_p}{n D_n + p D_p} \qquad (2)$$

U is the recombination rate, which, for an indirect band-gap semiconductor, is dominated by deep-level aided recombination. For a single deep-lying recombination center the Shockley-Read-Hall model[5] gives

$$U = \frac{np - n_i^2}{\tau_{po}(n + n_1) + \tau_{no}(p + p_1)} \qquad (3)$$

Since (2) and (3) are nonlinear functions of δp ($\delta p = p - p_o$, $\delta n = n - n_o$ and for quasi-neutrality $\delta p = \delta n$), Eq. (1) is nonlinear. In the low level injection limit ($\delta p/no \ll 1$), however,

$$D_a \to D_p,\ \mu_a \to \mu_p \text{ and } U \to \delta p/\tau_{po} \qquad (4)$$

resulting in a linear diffusion equation. In the high injection limit

$$\mu_a \to 0\ ,\ D_a \to D_\infty \text{ and } U \to \delta p/\tau_\infty \qquad (5)$$

and the ambipolar equation is again linear.

We have obtained analytical solutions of Eq. (1) for some special cases of interest by explicitly treating the nonlinear recombination and diffusion terms. The solutions we have obtained reduce to the well known solution in the low and high injection limits. The term involving E has been ignored in all the solutions, as is usually done[3], except one. This is justified because at low injection E is small. At higher levels of injection μ_a gets smaller (see Eq. 5 above) so that the term may still be ignored[6]. The various cases of interest are considered below.

1). Steady-State - Infinite Medium: This solution has been reported earlier[7]. It is of interest because it will be of use when considering steady-state diffusion. The solution is governed by

$$G = U \qquad (6)$$

and is given by

$$p_{ss} = \frac{1}{2}\left[-(n_o - \tau_\infty G) + \sqrt{(n_o - \tau_\infty G)^2 + 4\, n_o\, \tau_{po}\, G} \right] \qquad (7)$$

An approximate solution valid for small departure from low-injection, obtained by expanding (7) is

$$p_{ss} = \tau_{po} G \left(1 + \frac{\tau_{no} G}{n_o}\right) \qquad (8)$$

2). Time-Dependent Infinite Medium: For this case, the governing equation is

$$\frac{\partial \delta p}{\partial t} = G - U \qquad (9)$$

This equation can be solved explicitly.

3). Steady-State Diffusion: The steady-state diffusion case can be treated by introducing the change of variables[8]

$$y = \frac{d(\delta p)}{dx} \qquad (10)$$

This transformation leads to a first order nonlinear differential equation with variables separable. While complicated, the resulting equation can be integrated. A boundary condition is obtained by noting that

$$p(y = 0) = p_{ss} \qquad (11)$$

For reverse-bias, $p \approx 0$ at the depletion layer edge and the delayed component of photocurrent can be found by evaluating the current at the depletion-layer edge by Fick's Law,

$$J = q\, D_p\, y\, (p = 0) \qquad (12)$$

The full solution is plotted in Fig. 1 (curve labeled "Net") for $\tau_{no} = 10\ \tau_{po}$ and $D_n = 3\ D_p$. It is seen that photocurrent is a linear function of the dose rate for small and large values of G (low and high level injection limits) but becomes a superlinear function of G in the intermediate range of G.

J. Howard of RPI has incorporated into the device code PISCES-II[11] an ionization source to simulate LINAC irradiation. Initial results obtained with this code are consistent with the curve labelled "Net" in Figure 1 as shown in Figure 9.

Since two processes are involved in the departure from linearity, we have also considered them separately from each other. The effect of nonlinear recombination alone is found by solving (1) with U given by (3) and using $D_a = D_p$. The solution is plotted in Fig.1 (labeled "recombine") for $\tau_{no} = 10\ \tau_{po}$. It is seen that departure from low injection results in superlinear behavior of photocurrent when nonlinear recombination alone is considered. The appropriate expression for small departure from low level injection is obtained by expanding the solution in a Taylors series. This gives

$$J = J_o\ (1 + \frac{1}{3}\frac{\tau_{no} G}{n_o}) \qquad (13)$$

where J_o is the Wirth-Rogers current term ($J_o = -q\ GL_p$). It should be noted that the correction term in (13) is smaller than in (8). The steady-state carrier concentration rises more rapidly than the steady-state photocurrent at the onset of superlinearity, because low-level effects near the junction are imposed by boundary conditions even for high-injection cases.

The solution is plotted in Figure 1 (curve labeled "ambipolar"). For $D_n = 3D_p$. It is seen that for a p+n type of junction, ambipolar diffusion alone causes the photocurrent to become sublinear when departure from low level injection takes place. An expression for small departure from low injection for this case is

$$J = J_o\ [1 - \frac{1}{6}\frac{\tau_{po} G}{n_o}(1 - \frac{D_p}{D_n})] \qquad (14)$$

Since $D_p < D_n$ for silicon, the correction term is negative for a p+n junction. This is expected because electrons tend to diffuse ahead of holes which creates an electric field such that the slope of hole distribution at the depletion layer edge is reduced. A similar treatment of a n+p junction shows that, unlike in a p+n junction, the diffusion process tends to increase the photocurrent. The relative magnitude of the two effects is determined by the ratio D_n/D_p and τ_{no}/τ_{po}. For Si, $D_n/D_p \approx 3$ and $\tau_{no}/\tau_{po} \approx 1$ to 100. We have found that for this range of values of these parameters, the correction due to nonlinear recombination is always larger than the correction due to nonlinear diffusion in a p+n junction and therefore the photocurrent of a p+n junction can be approximated to first order by Eq. (13) when departure from low level injection takes place. This is illustrated in Fig. 2 which shows that the plot of Eq. (13) (labeled ""1st corr.") closely approxiates the plot of the exact solution for photocurrent (labeled "J_{net}" in the figure) for moderate departures from the low-level-injection where the Wirth and Rogers solution (labeled "W/R") is far from accurate. Both nonlinear recombination and diffusion have similar influence on the photocurrent in a n+p junction and both are small for $\tau_{no} > \tau_{po}$ and $D_n = 2$ to $3\ D_p$.

4). Steady-State Diffusion with Ohmic Field: Ohmic fields generally are neglected in low-injection problems[3]. An approximate model for evaluating $\partial(\delta p)/\partial x$ based on the Wirth-Rogers asymptotic form of solution has been used to estimate field effects. For most practical cases, the ohmic field effects are found to be small.

TRISPICE IMPLEMENTATION AND BIPOLAR DEVICE MODELING

Based on the various solutions presented earlier and the Wirth and Rogers transient photocurrent expression, we have implemented an approximate transient photocurrent expression in TRISPICE which is exact in limiting cases and should be a good approximation for moderate departure from low injection[9]. This approach is along lines similar to that used in Ref. [10] for treating hi-lo junctions.

Thus TRISPICE can now model photocurrent fairly accurately over the whole range of dose-rate corresponding to low, moderate and high level injection. The improved accuracy in the intermediate range of injection is especially significant because both the linear low-injection asymptotic solution and the linear high-injection asymptotic solution are inaccurate in this region. TRISPICE is capable of modeling finite device dimensions and the presence of high-low junctions[4] as in epi-CMOS. Secondary photocurrents are automatically accounted for by the active device models in the code.

The original geometry of the TRISPICE radiation model was designed to treat CMOS configurations[4]. A bipolar device model has been formulated. By redefining input parameters, it has been possible to have TRISPICE treat bipolar devices without internal code modifications. Our work with TRISPICE on bipolar Our work with TRISPICE on bipolar devices has so far concentrated on latchup modeling which usually involves parasitic bipolar devices. Such devices could have a geometry quite different from active bipolar devices and the TRISPICE photocurrent source parameters may have to be used in a different manner. However, we have found that in all cases studied to date we could fit the TRISPICE parameters to model the problem being considered.

LATCHUP ANALYSIS

We adopted data and practices from Ref. 2 to simulate a typical pnpn path. Specifically, a pnpn path in the monolithic 10 bit A/D converter AD571, which has been reported in Ref. 2, was chosen. The path was represented by the equivalent circuit of Fig. 7. Parameters for the radiation source and the bipolar junction transistors were inferred from the geometry of the path and the doping profile given in Ref. 2. The doping profile was approximated to be piecewise constant as shown in Fig. 8. With the transistor parameters that were used, we could reproduce the holding current reported for this pnpn path.

The simulation was first carried out by using a pre-calculated current source in SPICE along the lines of Ref. 2. We then repeated the same simulation with TRISPICE using both the linear and the extended version of the photocurrent source. When photocurrent is input as an external source, such as in SPICE, several difficulties arise such as uncertainty regarding the amplitude of the photocurrent, uncertainty regarding the rise-time and fall-time in the establishment of photocurrent, inability of the program to represent the actual time variation of the photocurrent, etc. For the sake of comparison, we selected the photocurrent amplitude in the SPICE-type run to be the same as we got from the TRISPICE run with a dose-rate of 2.1×10^9 rads/sec. SPICE has an exponential current source which we used and for which we selected the time-constant as the minority carrier lifetime. The result of the simulation is shown in Fig. 3. It is seen that the circuit latches and the voltage drops to a small value. The result of repeating the same simulation with TRISPICE (using the linear model) is shown in Fig. 4. Here it is seen that the voltage does not change significantly and the circuit does not latch. The difference in the two results, despite the fact that in both the cases photocurrent has the same amplitude, is attributable to the difference in the pulse shapes, and to the fact that latchup requires delivery of a critical charge while current is above the threshold current.

The two pulses are plotted in Fig. 5 for the sake of comparison. The TRISPICE pulse (dashed) rises more rapidly than the SPICE pulse (solid). The reason is the difference in the functional form of the two pulses. Thus despite the fact that the characteristic time in both the cases is the same, the TRISPICE pulse rises faster. The major difference in the two pulses, however, is that the TRISPICE pulse drops-off much more rapidly than does the SPICE pulse and thus has a smaller area above the threhold current than does the SPICE pulse. The charge threshold in this case lies between the area above the threshold current in the TRISPICE pulse and the SPICE pulse. Thus the SPICE pulse causes latchup while the TRISPICE pulse does not. The difference in rise and fall phase of the TRISPICE pulse is due to 3-D nature of the collection volume

$$VOL = \prod_{i=1}^{3} [A_i + B_i f_i(t)] \qquad (15)$$

In any time interval, the dimensions of the collection volume may be taken as a sum of a constant A_i representing drift and of a diffusion term with amplitude B_i and a time variation $f_i(t)$. For this case, diffusion dominates over drift and the B_i are larger than the A_i. When the pulse ends, drift ends abruptly, the volume varies as the product of the $f_i(t)$, and is characterized by a time constant shorter than that of the $f_i(t)$ themselves.

In situations where the drift component of photocurrent dominates and the pulse is narrow, the SPICE pulse has a lesser area and we have seen the opposite result, i.e., TRISPICE predicts latchup whereas SPICE does not. The point to emphasize, therefore, is that the result of explicit photocurrent modeling with TRISPICE can be significantly different from the results of modeling with a pre-determined current source and it may not always be possible to anticipate a subtle feature in the actual pulse shape and incorporate it beforehand in the precalculated current source. It is therefore important to carry out the simulation with improved and accurate photocurrent models so as to avoid misinterpretation of results.

We have previously seen that departure from low-level-injection can take place at fairly moderate dose-rates. Thus the photocurrent pulse shape and amplitude can start to change from that predicted by the linear model and this may influence latchup results. Two effects on the photocurrent pulse are expected to take place because of the increasing carrier lifetime with injection level (lifetime may also decrease with injection level under certain unusual situations). These are; increase in photocurrent magnitude over the linear case for the same dose-rate, as evidenced by the analytical expressions presented earlier, and, a slower rise and fall of the photocurrent pulse. For a sufficiently wide pulse, where photocurrent can reach its steady-state value, the result would be an increase in the integrated charge in the pulse which could exceed the charge threshold for latchup while the charge in the linear pulse may not. Thus the more accurate non-linear model may predict latchup when the linear model does not. Such a case has been observed by us. The case mentioned earlier, where TRISPICE (with linear model) did not predict latchup (Fig. 4) is repeated in Fig. 6 with the extended nonlinear photocurrent model. It is seen that photocurrent has a higher amplitude and caused the circuit to latch. On the other hand, for a sufficiently narrow pulse, it is possible for the nonlinear pulse to have lesser area than that predicted by the linear model. Therefore, once again, the point to emphasize is that the result of more accurate modeling could be substantially different from the results of simpler modeling and could either be more or less conservative. Thus one may be led to wrong conclusions and either over-designing or reducing hardness assurance because of inaccurate modeling.

CONCLUSIONS

Behavior of photocurrent has been analyzed when departure from low level injection takes place. Three factors tend to change the photocurrent from that predicted by Wirth and Rogers; nonlinear recombination, nonlinear diffusion and the presence of ohmic fields. The relative magnitude of these effects depends on the material type, its resistivity, the ratio D_n/D_p and τ_{no}/τ_{po} etc. It has been found that in a p+n type of junction the most significant effect is nonlinear recombination for $\tau_{no} > \tau_{po}$ and the other two effects can be ignored as compared to it. This effect is particularly large when $\tau_{no} \gg \tau_{po}$. In a n+p junction, however, both recombination and diffusion tend to make the photocurrent superlinear and both effects are small for $\tau_{no} > \tau_{po}$. The expression for moderate departure from low injection in this case is similar to the equivalent expression for a p+n junction[9]. Further work along these lines may involve investigation of other recombination mechanisms. For GaAs direct band-to-band recombination will have to be considered and, at very high dose-rates, Auger recombination will have to be taken into account for silicon.

It has also been demonstrated that explicit modeling of photocurrent using 3-D device representation and accurate models can lead to substantially differnt conclusions from those obtained in common practice with ordinary circuit analysis codes regarding the phenomenon of latchup and regarding the planning, conduct and interpretation of latchup tests.

REFERENCES

1. L. W. Nagel, "SPICE2: A Computer Program to Simulate Semiconductor Circuits," University of California-Berkeley Report ERL-M520, (1975).

2. R. L. Pease, D. R. Alexander, "pnpn Latchup in Bipolar Devices," Mission Research Corporation Report DNA6164F, (1982).

3. J. Wirth, S. Rogers, "Transient Response of Transistors and Diodes to Ionizing Radiation," IEEE Trans. Nuc. Sci., NS-11, p. 24 (1964).

4. L. W. Massengill, "The Implementation of a General Time and Voltage Dependent Current Source in the Circuit Simulation Program SPICE," MS Thesis, North Carolina University, (1984).

5. W. Shockley, W. Read, Jr., "Statistics of Recombination of Holes and Electrons," Phys. Rev. 87, p. 835, (1952).

6. J. P. McKelvey, "Solid State and Semiconductor Physics," Harper and Row, NY (1966).

7. J. S. Blakemore, "Semiconductor Statistics," Pergamon, NY (1962).

8. G. M. Margenau and G. M. Murphy, "Mathematics of Physics and Chemistry".

9. A. Ishaque, "Response of Reverse Biased P-N Junctions to Moderate and Strong Intensity Ionizing Radiation," MS Thesis, Rensselaer Polytechnic Institue, (1986).

10. D. Long, J. Florian, R. Casey, "Transient Response Model for Epitaxial Transistors," IEEE Trans. Nuc. Sci, NS-30, P. 4131 (1983).

11. M. R. Pinto, C. S. Rafferty, R. W. Dutton, "PISCES II: Poisson and Continuity Equation Solver," Stanford Electronics Laboratories, 1984.

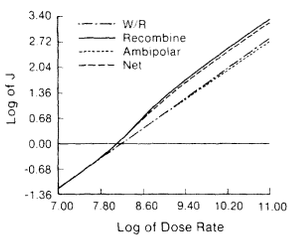

Fig. 1 Comparison of the photocurrent model which includes non-linear recombination and non-linear diffusion (curve labelled "Net") with the models which include non-linear recombination alone (curve labelled "Recombine") and non-linear diffusion alone (curve labelled "Ambipolar")

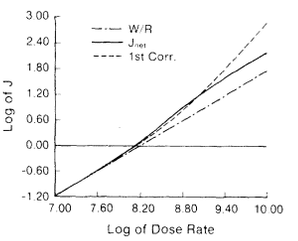

Fig. 2 Comparison of the approximate recombination model with the model which includes all the effects

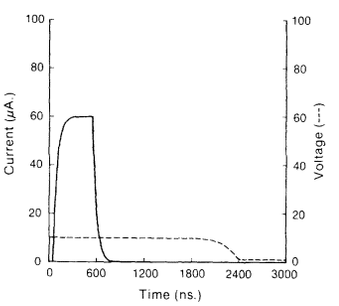

Fig. 3 SPICE simulation of a pnpn path

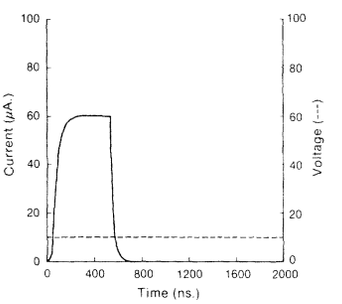

Fig. 4 TRISPICE simulation of a pnpn path with the linear model

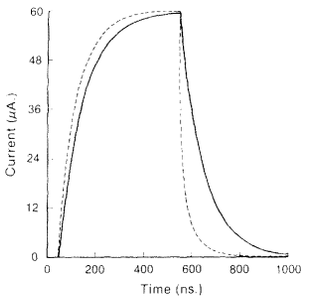

Fig. 5 Comparison of TRISPICE (dashed) and SPICE (solid) pulses

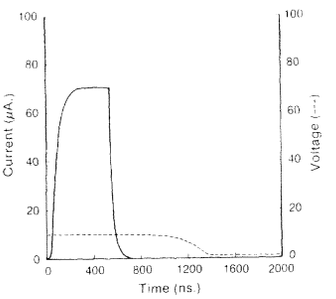

Fig. 6 TRISPICE simulation of a pnpn path with the extended model

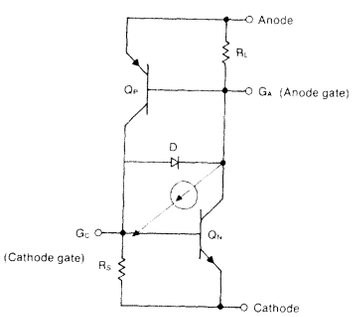

Fig. 7 Equivalent circuit for a pnpn path

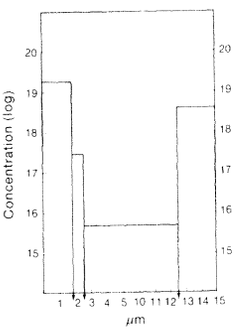

Fig. 8 Doping profile for the pnpn path that was simulated

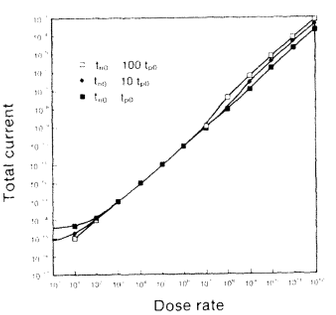

Fig. 9 Pisces results